Journal of the Mechanical Behavior of Materials

Mokarram Hossain · A. F. M. S. Amin · Muhammad Nomani Kabir

Eight-chain and full-network models and their modified versions for rubber hyperelasticity : A comparative study

Received: date / Accepted: date

Abstract The eight-chain model (Arruda EM, Boyce MC, 1993. A three-dimensional constitutive model for the large stretch behaviour of rubber elastic materials. J. Mech. Phy. Solids 41, 389-412), also known as Arruda-Boyce model, is widely used to capture the rate-independent hyperelastic response of rubberlike materials. The parameters of this model are physically based and explained from micromechanics of chain molecules. Despite its excellent performance with only two material parameters to capture bench measurements in uniaxial and pure shear regime, the model is known to be significantly deficient in predicting the equibiaxial data. To ameliorate such drawback, over the years, several modified versions of this successful model have been proposed in the literature. The so-called full-network model is another micromechanically-motivated chain model, which has also few modified versions in the literature. For this study, two modified versions of the full-network model have been selected. In this contribution, five modified versions of the Arruda-Boyce model and two modified versions of full-network model are critically compared with the classical eight chain model for their adequacy in representing equibiaxial data. To do a comparison of all selected models in reproducing the well-known Treloar data (Trans Faraday Soc 40:59-70, 1944), the analytical expressions for the three homogeneous deformation modes, i.e. uniaxial tension, equibiaxial tension and pure shear have been derived and the performances of the selected models are analysed. The comparative study

Mokarram Hossain
Chair of Applied Mechanics, University of Erlangen-Nuremberg, Germany
Tel.:+49-9131-8528514
Fax: +49-9131-8528503
E-mail: mokarram.hossain@ltm.uni-erlangen.de
A. F. M. S. Amin
Department of Civil Engineering, Bangladesh University of Engineering and Technology, Dhaka, Bangladesh
Tel.: +880-2-8616833, Ext 7944
E-mail: samin@ce.buet.ac.edu
Muhammad Nomani Kabir
Department of Computer Science, Taibah University, Madinah, Saudi Arabia
E-mail: dr.nomankabir@gmail.com

demonstrates that modified Flory-Erman model, Gornet-Desmorat (GD) model, Meissner-Matějka model and Bootstrapped eight-chain model predict well the three deformation modes compare to the classical eight-chain model.

Keywords Eight-chain model · Full-network model · Rubber-like material · Phenomenological model · Micromechanical model

1 Introduction

Rubber-like materials have enormous applications especially in industrial and engineering fields, such as tires, engine mounts, seals, conveyor belts, base isolations for protecting buildings and bridges from devastating earthquakes [1; 2; 3; 4; 37]. Such wide-range of applications of rubbers make the rubber-mechanics as one of the major active fields of research in last several decades. Especially the fast growing numerical techniques such as the finite element method facilitate sophisticated design and analysis for complex large strain three-dimensional elastomeric components. In the development of numerical models, a simple but advanced constitutive model to capture multi-axial data is an essential ingredient. The large deformability together with recoverability of rubber-like materials are well known for their highly nonlinear load-deformation behaviour. These materials are generally modelled by considering homogeneous, isotropic, incompressible or nearly incompressible, geometrically and physically nonlinear (visco) elastic solids. Such idealizations are also supported by experimental data [15; 27].

In the literature [9; 26], elastomeric material models are generally classified into two main categories: purely *phenomenological* and *micromechanical* based network models. The micromechanically-motivated network models, on the one hand, are based on the statistics of cross-linked long chain molecules [9] and the phenomenological models, on the other hand, involve invariant or principal stretch-based macroscopic continuum formulations generally having polynomial structures. The governing parameters appearing in the proposed expressions of the energy functions of the phenomenological models do not have, in most of the cases, any physical interpretation. The three-chain, four-chain, eight-chain, full network models, tube-model, extended-tube model, Flory-Erman model, micro-macro unit sphere model, Kroon model are well-known micromechanically-inspired models, which can be used for moderate to large elastic deformations of polymeric materials, see for example, Boyce and Arruda [9], Arruda and Boyce [11], Miehe et al. [8], Hossain and Steinmann [26]. Some well-known phenomenological models are Neo-Hooke, Mooney-Rivlin, Ogden, Gent, Yeoh, Attard, Shariff, Hart-Smith, van der Waals, Lopez-Pamies, Pucci-Saccomandi, Carroll etc, for more details, see Hossain and Steinmann [26], Steinmann et al. [28].

As mentioned earlier, numerous constitutive models have been proposed during the last several decades to describe the elastic response of elastomers, but only a few of them are able to satisfactorily reproduce ex-

perimental data for different deformation modes, i.e. uniaxial and biaxial extensions, simple and pure shears. According to Marckmann and Verron [16], the promising candidate for the best model will be that one, which can describe the complete behaviour of elastomers with a minimal number of material parameters that can be determined from explicit experimental data without facing any difficulty, e.g. instability. Marckmann and Verron [16], after comparing twenty models, placed the extended tube model [17], Shariff model [23], micro-macro unit sphere model [8] and Ogden [12; 13] model at the top of their ranking list. Earlier, Boyce and Arruda [9] conducted an excellent review on several hyperelastic models where they utilized Treloar's experimental data for comparison of three type of deformations (uniaxial, biaxial and pure shear).

The eight-chain model is a classical micromechanically-motivated constitutive model for polymeric materials, where the governing parameters have direct links to the micro-mechanics of the polymer molecular structures. With only two material constants, this model excellently captures major classical experimental data available in the literature. Despite its excellent performance to capture the uniaxial and pure shear data in the case of Treloar, the model prediction faces a significant deficiency to calibrate the equibiaxial data [9; 32]. Several modified versions of this model were proposed over the last two decades to show a better performance in the equibiaxial range. Some variants are of structural types while the extended or modified parts of some other variants are based purely on phenomenological consideration, cf. [30]. For the sake of modifications over the classical one, some models increase the number of parameters to fit the data, e.g. Bechir model [33] while some remain with the two parameters, e.g. Bootstrapped eight-chain model [32]. Some well-known modified versions of the Arruda-Boyce model are: modified Flory-Erman model [9; 21], Gornet-Desmorat (GD) model [30], Bootstrapped eight-chain model [32], Bechir model [33], Meissner-Matejka model [34], Kroon model [15]. When a modified model is proposed aiming to show better results in contrast to the original eight-chain model, the modified version is usually compared with the original one but the comparison among the variants of the eight-chain model are not demonstrated so far in the literature. Therefore, such comparative study can work as a guideline for a beginner who wants to work in rubber mechanics to choose an appropriate model from several variants.

The full-network model is also a micromechanically-inspired model where polymer chains are assumed to be randomly oriented in space. Due to the computational cost for the integration over a sphere, either analytically or numerically, several simplified approaches for this model have been proposed in the literature [14; 24; 36] where analytical or numerical integration over the sphere is bypassed. For this study, we have selected the modified full-network model due to Wu and Giessen [14] and the another one that is proposed in Zuniga and Beatty [24]. The aim of the current study is to present a comparative study among all modified versions so far available in the literature, at least to the best of the author's knowledge.

The paper is structured as follows: in Section 2 we briefly review the general framework for the derivation of (semi) analytical stress-strain relations from arbitrary free energy functions for the homogeneous cases. In

Section 3, the analytical formulations for the three homogeneous deformation modes, i.e. uniaxial tension, equibiaxial tension and pure shear are derived for all selected models. These are necessary to evaluate the performance of all chosen models in reproducing the experimental data provided by Treloar. To this end a standard fitting tool is applied to calculate the optimal model parameters with respect to each set of Treloar's data. Section 3 also presents a comparative study on six modified models along with the original eight-chain and full-network models. Finally concluding remarks close the paper.

2 Analytical formulations

Concerning comparison of a novel model with the existing one (s), most of the authors used constitutive (semi) analytical expressions and the classical Treloar data. Since these data are given in pairs of principal stretches λ_i and principal 1^{st}-Piola-Kirchhoff (PK) stresses P_i for different deformation modes, e.g. uniaxial tension (UN), equibiaxial tension (EB) and pure shear (PS), the analytical formulations for the principal 1^{st}-Piola-Kirchhoff (PK), i.e. $P_i(\lambda_i)$ need to be derived from the particular free energy function. Then, in order to compare the analytical expression with the experimental data, an optimal set of material parameters for each model and a particular deformation mode has to be identified. For the parameter identification, different optimization techniques can be used. The material investigated by Treloar is characterised as isotropic and incompressible, a case for which principal stretches and 1^{st}-PK stresses are related by

$$P_i = \frac{\partial \Psi}{\partial \lambda_i} - \frac{1}{\lambda_i} p \quad , \quad i = 1, 2, 3 \text{ (no sum)} \tag{1}$$

where p denotes the hydrostatic pressure that has to be determined from appropriate boundary conditions, for details see [9; 26]. For the case of invariant based models, i.e. $\Psi = \tilde{\Psi}(I_1, I_2)$, the equation (1) leads to

$$P_i = \frac{\partial \Psi}{\partial I_1}\frac{\partial I_1}{\partial \lambda_i} + \frac{\partial \Psi}{\partial I_2}\frac{\partial I_2}{\partial \lambda_i} - \frac{1}{\lambda_i} p \quad , \quad i = 1, 2, 3 \text{ (no sum)}. \tag{2}$$

Using Eqns (1) and (2) we derive the required analytical formulations for the three homogeneous deformation modes. For further details, see Hossain and Steinmann [26], Steinmann et al. [28]. To identify the material parameter set for each model, an open source computer code, `TRESNEI` is used. The code is suitable for bound-constrained non-linear least-square problems, cf. [29]. For the validation of each model, each set of optimal material parameters for UN, EB and PS is used to compute the response of the other two deformation modes. Each subsection contains the corresponding figures that also contain the errors between (a) each experiment and its optimal fit, e.g. Error(UN-fit), and (b) the simulations of the other deformation modes and their respective measurements, e.g. Error(EB-sim). All error calculations have been performed according to the relation below

$$\text{Error(fit/sim)} = \sqrt{\frac{1}{M}\sum_{i=1}^{M}\left[P_{\text{fit/sim}}(\lambda_i^{\text{Treloar}}) - P_{\text{Treloar}}(\lambda_i^{\text{Treloar}})\right]^2}, \tag{3}$$

i.e. sum up the squared differences between fitted/simulated and measured first Piola-Kirchhoff stresses, respectively, averaged by the number of data points M (stretches) available for each deformation mode.

3 Comparative study: Model performances

3.1 Eight-chain model

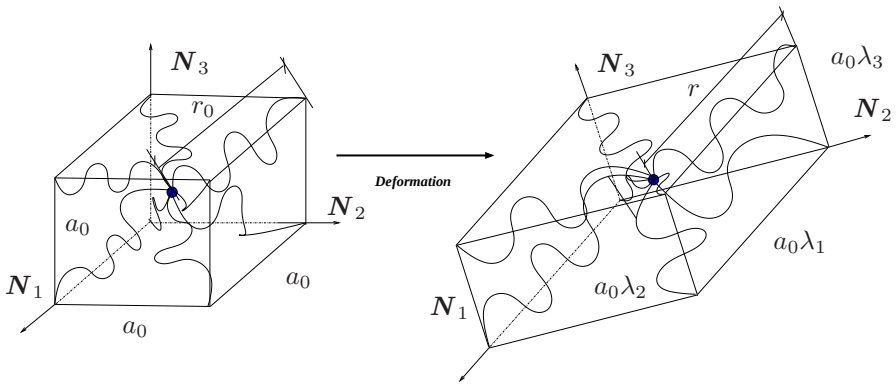

Fig. 1 Eight-chain model: initial and deformed chain orientations and stretches

In this model, the cuboid volume element, cf. Fig (1) is assumed to have edges parallel to the principal directions, which is composed of eight chains (hence the name eight-chain model) oriented in the diagonals from the center of the volume to its corners. The relation between edge length a_0 of the cuboid and the chain length r_0, in the undeformed state, is given by simple geometric relations, $a_0 = \frac{2}{\sqrt{3}} r_0$, wherein $r_0 = l\sqrt{N}$ is denoted as the end-to-end distance of an unstretched chain. In current deformed state it reads: $r = r_0\sqrt{3^{-1}}\sqrt{\lambda_1^2+\lambda_2^2+\lambda_3^2}$, where $\lambda_1, \lambda_2, \lambda_3$ are the principal stretches of the right Cauchy-Green tensor $\boldsymbol{C} = \boldsymbol{F}^T\boldsymbol{F}$, $\boldsymbol{F}$ being the deformation gradient. By defining the mean value of the stretch λ_c, which is required to determine the expression for the macroscopic free energy, we obtain

$$\lambda_c = \frac{r}{r_0} = \sqrt{\frac{1}{3}\left[\lambda_1^2+\lambda_2^2+\lambda_3^2\right]} = \sqrt{\frac{I_1}{3}}. \tag{4}$$

In Eqn (4), I_1 is the first invariant of $\boldsymbol{C}$, i.e. $I_1 = \text{tr}\boldsymbol{C}$. Inserting the Langevin statistics of a single chain, the free energy can be obtained as

$$\Psi_{8ch} = \mu N \left[\gamma \lambda_{c,r} + \ln \left(\frac{\gamma}{\sinh \gamma} \right) \right], \tag{5}$$

with the relative chain stretch $\lambda_{c,r} = \frac{\lambda_c}{\sqrt{N}} = \sqrt{\frac{I_1}{3N}}$, where μ, N, γ are the shear modulus, the number of chain segments per chain and the inverse Langevin function, respectively. It is revealed that this model accurately captures the ultimate strain of network deformation while requiring only two material parameters, the shear modulus (μ) and the number of segments per chain (N). Due to the inherent micromechanical explanations in defining these two material parameters, such constitutive framework is often referred a micromechanically-motivated model.

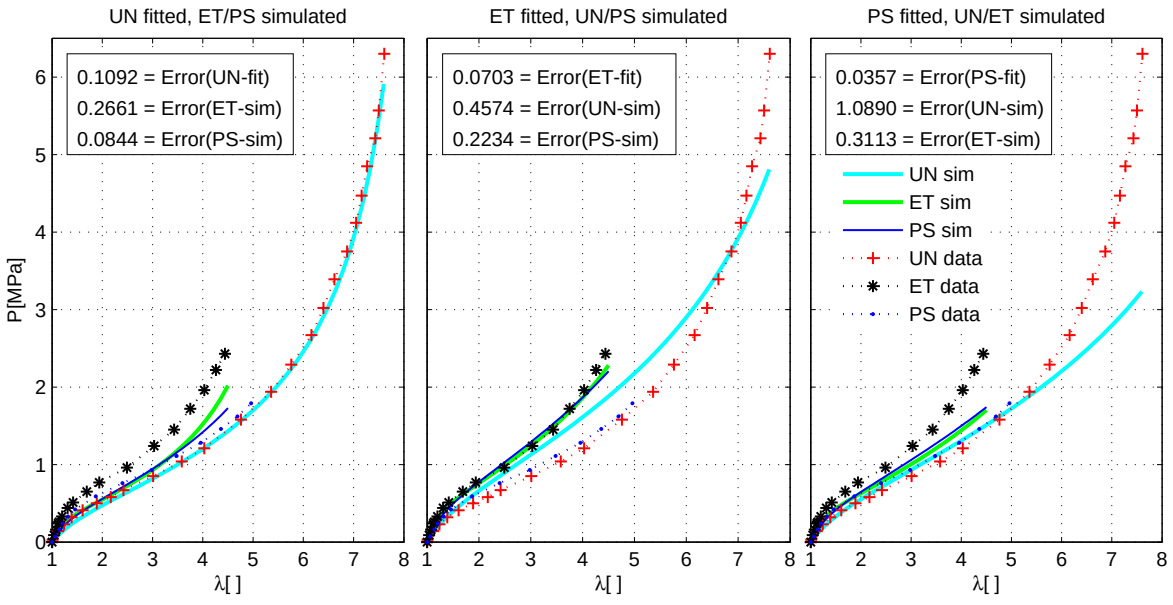

Fig. 2 Performance of the eight-chain model on the Treloar data. The fittings and simulations in two deformation modes (UN and EB) are good to excellent except in the pure shear case where the prediction fails to reproduce the S-shape of uniaxial case at high strains. Uniaxial simulation and fitting are almost concident (**left**) while equibiaxial simulation overestimates the Treloar data.

The analytical $P_i(\lambda_i)$-relations for the three deformation modes UN, EB and PS, which are required to check the performance of the model on the Treloar data, are obtained from Eqn (1) as

$$P_1^{UN} = \frac{\mu^{UN}}{3}\left[\frac{3N^{UN}-\lambda_{cu}^2}{N^{UN}-\lambda_{cu}^2}\right]\left[\lambda-\lambda^{-2}\right], \quad \lambda_{cu} = \sqrt{\frac{1}{3}\left[\lambda^2+\frac{2}{\lambda}\right]} \tag{6}$$

$$P_{1,2}^{EB} = \frac{\mu^{EB}}{3}\left[\frac{3N^{EB}-\lambda_{cb}^2}{N^{EB}-\lambda_{cb}^2}\right]\left[\lambda-\lambda^{-5}\right], \quad \lambda_{cb} = \sqrt{\frac{1}{3}\left[2\lambda^2+\frac{1}{\lambda^4}\right]} \tag{7}$$

$$P_1^{PS} = \frac{\mu^{PS}}{3}\left[\frac{3N^{PS}-\lambda_{cp}^2}{N^{PS}-\lambda_{cp}^2}\right]\left[\lambda-\lambda^{-3}\right], \quad \lambda_{cp} = \sqrt{\frac{1}{3}\left[\lambda^2+\lambda^{-2}+1\right]}. \tag{8}$$

Note that in approximating the inverse Langevin function (γ), the Padé approximation is applied due to its superior performance over other approximation procedures, i.e. $\gamma = \mathscr{L}^{-1}(\lambda_{c,r}) \approx \lambda_{c,r}\frac{3-\lambda_{c,r}^2}{1-\lambda_{c,r}^2}$, cf. [8]. By calibrating the UN, EB and PS equations to the corresponding Treloar data, the optimal material parameters are estimated:

$$\mu^{UN} = 0.264 \text{ MPa}, \qquad \mu^{EB} = 0.358 \text{ MPa}, \qquad \mu^{PS} = 0.311 \text{ MPa},$$
$$N^{UN} = 25.60, \qquad N^{EB} = 30.26, \qquad N^{PS} = 51.32.$$

The optimal material parameters obtained by using analytical expressions are utilized to simulate the experimental data of the other two deformation modes and their corresponding errors with respect to the Treloar data are calculated. The results, cf. Fig (2) are obtained by inserting the Padé approximation of the inverse Langevin function in the free energy function. It is clear from the Fig (2) that with a least number of material parameters, i.e. two, this model produces better results in all deformation modes.

3.2 Modified Flory-Erman model

In most of the micromechanically-inspired models, authors derive the energy functions by considering only the contributions from the cross-linking of polymer chains while the contributions due to entanglements have been neglected. Boyce and Arruda [9] proposed a modification of their original model by adding a constraint term devised by Flory and Erman [21]. The assumption of Flory and Erman is that a long macromolecule network consists of numerous chain connection points, which are constrained from phantom characteristics due to the presence of neighbouring chains. As a result, the elastic strain energy of the network is originated from two contributions, i.e. the phantom (Ψ_{ph}) and the topological constraint (Ψ_{ct}) contributions as

$$\Psi = \Psi_{ph} + \Psi_{ct}. \tag{9}$$

Flory and Erman [21] derived the phantom part of the energy function from the Gaussian chain statistics, equivalent to the Neo-Hookean case, i.e. $\Psi_{ph} = \sum_{i=1}^{3}\frac{\mu}{2}[1-\frac{1}{\phi}][\lambda_i^2-1]$ and the constraint part is obtained

from the micromechanics of the chain molecules as

$$\Psi_{ct} = \sum_{i=1}^{3} \frac{\mu}{2}\Big[B_i + D_i - \ln(B_i+1) - \ln(D_i+1)\Big] \tag{10}$$

with $B_i = \kappa^2[\lambda_i^2-1][\lambda_i^2+\kappa]^{-2},\ D_i = \lambda_i^2\kappa^{-1}B_i$. In Eqn (10), the parameter μ represents the shear modulus, ϕ counts the number of chains joining at a junction and κ measures the strengths of the constraints, respectively. Since the Flory-Erman model at large stretches deviates significantly from the actual response of the networks due to the Gaussian nature of its phantom part, Boyce and Arruda [11] applied their eight-chain energy function for the phantom part to improve the overall response, which, we designate here as the modified Flory-Erman model. Replacing the Neo-Hookean part by the eight-chain energy function, the modified Flory-Erman model yields

$$\begin{aligned}\Psi &= \Psi_{8ch} + \Psi_{ct} \\ &= \mu N\left[\gamma\lambda_{c,r} + \ln\left(\frac{\gamma}{\sinh\gamma}\right)\right] + \sum_{i=1}^{3}\frac{\mu}{2}\Big[B_i + D_i - \ln(B_i+1) - \ln(D_i+1)\Big]\end{aligned} \tag{11}$$

where $\mu, N, \gamma, \lambda_{c,r}$ are defined in Section 3.1.

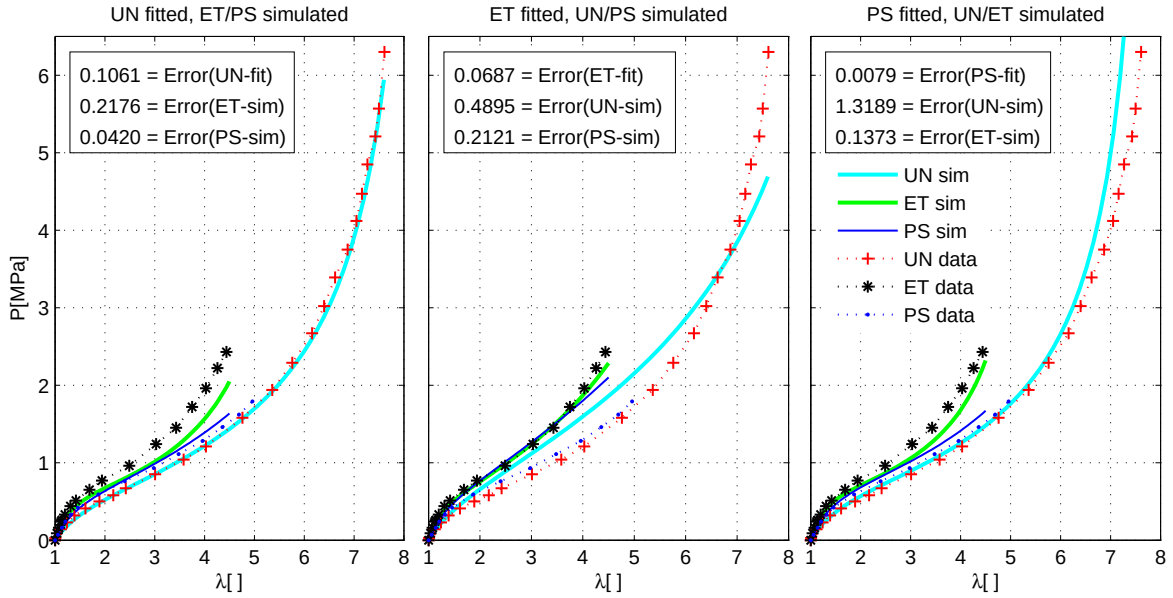

Fig. 3 Performance of the Flory-Erman model modified by the eight-chain energy function on the Treloar data. The fitting quality and predictions are excellent, especially if compared to the similarly structured models, e.g. the original eight-chain model or the Gent model, cf. Steinmann et al. [28].

The constraint contribution of the stress-stretch relations has to be derived from the single differentiation of the constraint part of the energy function appearing in Eqn (11) and is demonstrated in Appendix A. If the

analytical expressions for UN, EB and PS fit to the corresponding Treloar data, the optimal material parameter sets are found to be

$$\begin{aligned}\left[\mu^{UN}, N^{UN}, \kappa^{UN}\right] &= [0.251 \text{ MPa}, 25.46, 2.0] \\ \left[\mu^{EB}, N^{EB}, \kappa^{EB}\right] &= [0.363 \text{ MPa}, 37.75, 0.011] \\ \left[\mu^{PS}, N^{PS}, \kappa^{PS}\right] &= [0.24 \text{ MPa}, 22.07, 5.323]\,.\end{aligned}$$

Each of the parameter sets is used to simulate the experimental data of other two deformation modes. The results are plotted in Fig (3) as well as the corresponding errors from both fitting and simulation of experiments not used for the parameter identification. In comparison to the original eight-chain model, it is interesting to note that the inclusion of the constraint contribution to the eight-chain energy function improves the simulation for the EB in all three deformation cases as well as the simulations for UN and EB by the PS-fitted parameters, cf. Fig 3 (**right**). A small drawback of the modified model is, the additional contribution for the topological constraint yields a complicated lengthy expression for the stress-stretch relationships, see Appendix A.

3.3 Gornet-Desmorat (GD) model

To improve the prediction capability in multi-axial loadings for rubber-like materials, very recently Gornet et al. [30] proposed a strain energy function based on the first and second strain invariants of the right Cauchy-Green tensor. The first part is dependent on the first invariant and it corresponds to the Hart-Smith model. The equivalence between the eight-chain model and I_1-dependent part of the Hart-Smith model is established by Chagnon et al. [19]. To enhance the phantom network, i.e. the cross-link part expressed by the first invariant I_1, an additional function based on I_2 is added to the energy function. Gornet et al. [30] show that such addition will constrain the eight-chains by a new network of chains on the surfaces of the cube, which mimics the behaviour of the constraint contribution. Finally, the energy function of the GD model is expressed as

$$\Psi = h_1 \int e^{h_3[I_1-3]^2} dI_1 + 3h_2 \int \frac{1}{\sqrt{I_2}} dI_2 \tag{12}$$

where h_1, h_2, h_3 are material parameters. Evaluation of Eqn (2) provides the corresponding analytical formulations for the UN, EB and PS cases:

$$P_1^{UN} = 2\left[h_1 e^{h_3[I_1-3]^2} + \frac{3h_2}{\lambda\sqrt{I_2}}\right]\left[\lambda - \lambda^{-2}\right] \tag{13}$$

$$P_{1,2}^{EB} = 2\left[h_1 e^{h_3[I_1-3]^2} + \frac{3h_2\lambda^2}{\sqrt{I_2}}\right]\left[\lambda - \lambda^{-5}\right] \tag{14}$$

$$P_1^{PS} = 2\left[h_1 e^{h_3[I_1-3]^2} + \frac{3h_2}{\sqrt{I_2}}\right]\left[\lambda - \lambda^{-3}\right]. \tag{15}$$

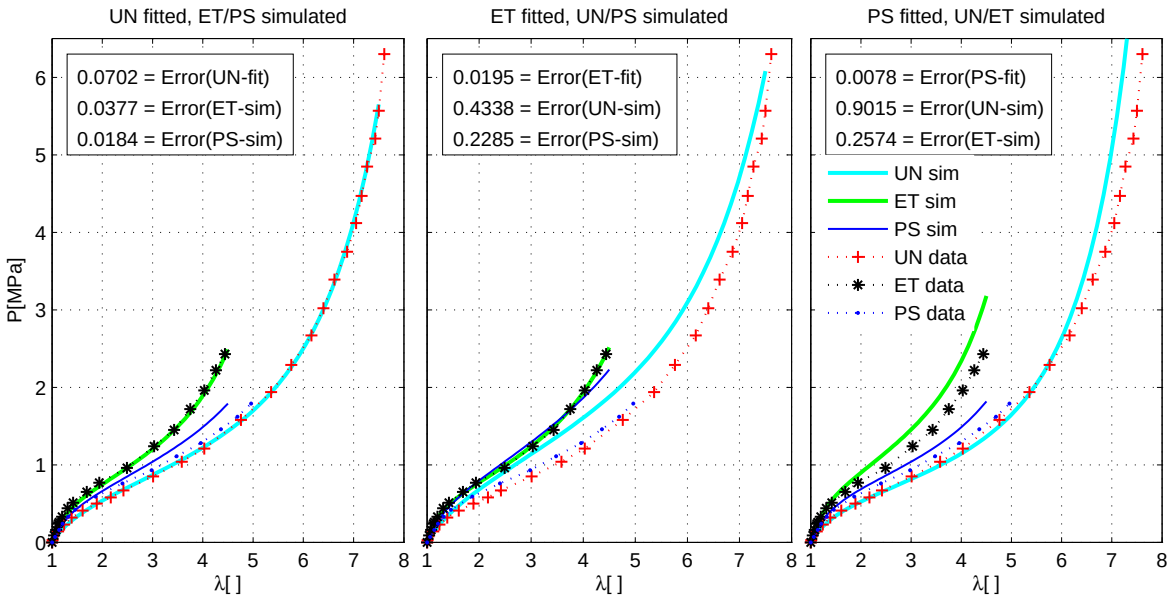

Fig. 4 Comparison between the GD model and the Treloar data. Fitting to the analytical formulations and model prediction quality are excellent, especially in UN and PS. Only predictions for the EB-fitted parameters overestimate the UN and PS data.

By calibrating the UN, EB and PS equations to the corresponding Treloar data, the optimal material parameters are found:

$$h_1^{UN} = 0.142 \text{ MPa}, \quad h_1^{EB} = 0.194 \text{ MPa}, \quad h_1^{PS} = 0.124 \text{ MPa},$$

$$h_2^{UN} = 1.58\text{e-}2 \text{ MPa}, \quad h_2^{EB} = 2.0\text{e-}14 \text{ MPa}, \quad h_2^{PS} = 0.034 \text{ MPa},$$

$$h_3^{UN} = 3.49\text{e-}4, \quad h_3^{EB} = 2.56\text{e-}4, \quad h_3^{PS} = 4.94\text{e-}4.$$

For validity of this model, each parameter set obtained from the optimization tool is used to simulate the other two deformation modes. The results are plotted in Fig (4) together with fitting and simulation errors in each case. It can clearly be shown here that the simulations for the EB and PS by the UN-fitted parameters produce results that are quantitatively much more acceptable than any other of the previous models with the same number of parameters, cf. Figs (4, **left**) and (4, **right**). The simulations for the EB-fitted parameters

overestimate the UN and PS data, cf. Fig (4, **middle**) while the predictions for the PS-fitted parameters are good to fair, cf. Fig (4, **right**).

3.4 Bootstrapped eight-chain model

In an attempt to improve the results for the eight-chain model at small strain, a new model called bootstrapped eight-chain model with only two material parameters (same as in the original eight-chain model) is proposed by Miroshnychenko and Green [31; 32]. They further assume that, in order to improve results especially in the biaxial deformation, an additive form of the strain energy function that involves two functions-one depends on the first invariant and the other on the second invariant of a deformation tensor, has to be formulated. Such an assertion is also supported by Pucci and Saccomandi [25], Hart-Smith [20]. The full strain energy function of the bootstrapped eight-chain model is written as:

$$\Psi = \Psi_{8ch}\left(\frac{i_1}{\sqrt{3N}} - \frac{\lambda_c}{\sqrt{N}}\right) + \Psi_{8ch}\left(\frac{\lambda_c}{\sqrt{N}}\right) \tag{16}$$

where $i_1 = \lambda_1 + \lambda_2 + \lambda_3$ and the definitions of λ_c, N are given in Section 3.1. For the complete expression of the eight-chain model, previous subsection is referred. The energy function from Eqn (16) yields three principal stresses as

$$\sigma_i = \mu\sqrt{N}\left[\frac{\lambda_i}{\sqrt{3}} - \frac{\lambda_i^2}{3\lambda_c}\right]\mathscr{L}^{-1}\left(\frac{i_1}{\sqrt{3N}} - \frac{\lambda_c}{\sqrt{N}}\right) + \mu\sqrt{N}\left[\frac{\lambda_i^2}{3\lambda_c}\right]\mathscr{L}^{-1}\left(\frac{\lambda_c}{\sqrt{N}}\right). \tag{17}$$

Using Eqn (17), the analytical formulations for the three different deformation modes, i.e. UN, EB and PS are derived as

$$P_1^{UN} = \frac{\mu^{UN}}{\lambda}\lambda_u\frac{3N^{UN} - \lambda_u^2}{N^{UN} - \lambda_u^2}\left[\frac{\lambda - \lambda^{-1/2}}{\sqrt{3}} - \frac{\lambda^2 - \lambda^{-1}}{3\lambda_{cu}}\right] + \frac{\mu^{UN}}{3}\left[\frac{3N^{UN} - \lambda_{cu}^2}{N^{UN} - \lambda_{cu}^2}\right]\left[\lambda - \lambda^{-2}\right] \tag{18}$$

$$P_{1,2}^{EB} = \frac{\mu^{EB}}{\lambda}\lambda_b\frac{3N^{EB} - \lambda_b^2}{N^{EB} - \lambda_b^2}\left[\frac{\lambda - \lambda^{-2}}{\sqrt{3}} - \frac{\lambda^2 - \lambda^{-4}}{3\lambda_{cb}}\right] + \frac{\mu^{EB}}{3}\left[\frac{3N^{EB} - \lambda_{cb}^2}{N^{EB} - \lambda_{cb}^2}\right]\left[\lambda - \lambda^{-5}\right] \tag{19}$$

$$P_1^{PS} = \frac{\mu^{PS}}{\lambda}\lambda_p\frac{3N^{PS} - \lambda_p^2}{N^{PS} - \lambda_p^2}\left[\frac{\lambda - \lambda^{-1}}{\sqrt{3}} - \frac{\lambda^2 - \lambda^{-2}}{3\lambda_{cp}}\right] + \frac{\mu^{PS}}{3}\left[\frac{3N^{PS} - \lambda_{cp}^2}{N^{PS} - \lambda_{cp}^2}\right]\left[\lambda - \lambda^{-3}\right]. \tag{20}$$

In Eqns (18-20), $\lambda_u = \frac{i_{1u}}{\sqrt{3}} - \lambda_{cu}$, $\lambda_b = \frac{i_{1b}}{\sqrt{3}} - \lambda_{cb}$, $\lambda_p = \frac{i_{1p}}{\sqrt{3}} - \lambda_{cp}$, $i_{1u} = \lambda + 2\lambda^{-1/2}$, $i_{1b} = 2\lambda + \lambda^{-2}, i_{1p} = \lambda + \lambda^{-1} + 1$ and $\lambda_{cu}, \lambda_{cb}, \lambda_{cp}$ are defined in Eqns (6-8).

Fitting the analytical equations (18-20) to Treloar's data yields the following parameter sets

$$\begin{aligned} &\mu^{UN} = 0.277 \text{ MPa}, && \mu^{EB} = 0.318 \text{ MPa}, && \mu^{PS} = 0.322 \text{ MPa}, \\ &N^{UN} = 26.50, && N^{EB} = 30.11, && N^{PS} = 72.18. \end{aligned}$$

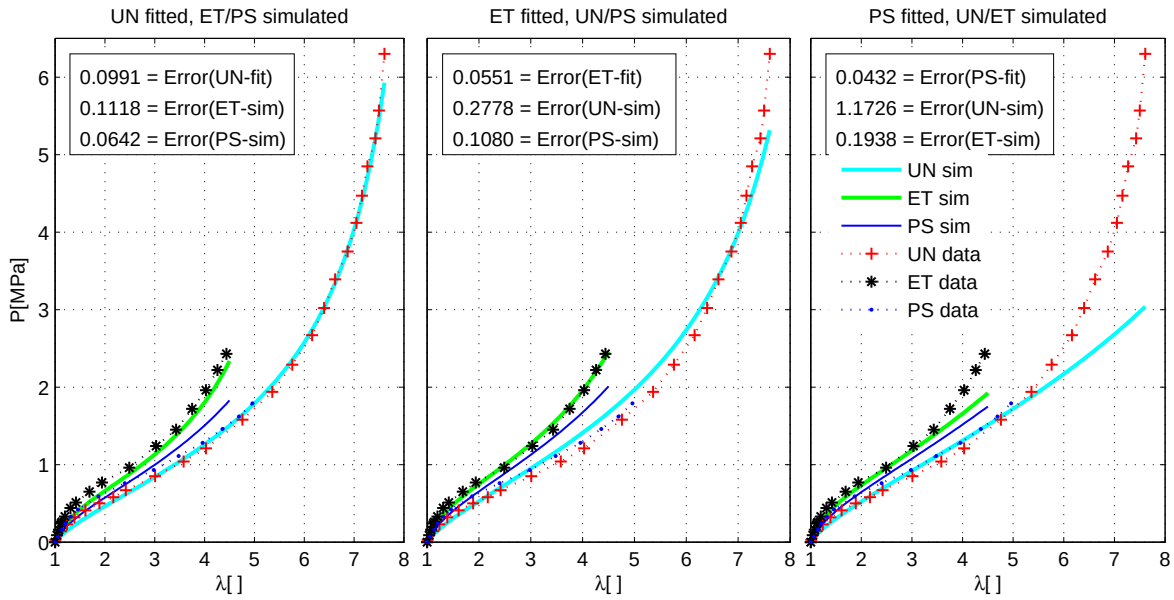

Fig. 5 Performance of the Bootstrapped eight-chain model on the Treloar data. The fittings and simulations are good to excellent, especially if compared to the similarly structured models, e.g. the original eight-chain model or the two-parameter Gent model.

Figure (5) depicts all fits, the simulations of complementary deformation modes that are not used during optimization and the deviations in comparison to the Treloar's data. Both fitting quality and validity of the identified parameters are very good to excellent in the UN and EB-cases. Optimization with respect to the PS-data provides parameter sets that fail to predict the UN-data, cf. Fig (5, **right**). Similar to the classical eight-chain model, the bootstrapped model also fails to predict the S-shape in the case of UN for PS-fitted parameters. After analysing the errors, fittings and the validation results, it can be concluded that with the same number of parameters, the bootstrapped eight-chain model illustrates better performance in all deformation modes than the classical eight-chain model.

3.5 Meissner-Matějka model

Based on the fact that to cope with the experimental data, not only the contribution from the cross-link part but also a constraint term in the energy function is essential. Meissner and Matějka [34; 35] proposed an energy function where the cross-link term is derived from the structure-based Arruda-Boyce model and the constraint part is based on the first invariant of the generalized deformation tensor. Note that here the constraint part is exactly same as the constraint part in the extended tube model proposed by Kalikse and Heinrich [18]. Then, the total energy function is expressed:

$$\Psi = \mu N \left[\gamma\lambda_{c,r} + \ln\left(\frac{\gamma}{\sinh\gamma}\right)\right] + \sum_{i=1}^{3} \frac{2\mu_e}{\beta^2}\left[\lambda_i^{-\beta} - 1\right] \tag{21}$$

where μ, N, μ_e, β $(0 < \beta \leq 1)$ are material parameters. The definitions of $\lambda_{c,r}, \gamma$ are given in Section 3.1. Evaluation of Eqn (1) provides the corresponding analytical formulations for the UN, EB and PS cases:

$$P_1^{UN} = \frac{\mu^{UN}}{3}\left[\frac{3N^{UN} - \lambda_{cu}^2}{N^{UN} - \lambda_{cu}^2}\right]\left[\lambda - \lambda^{-2}\right] + \frac{2\mu_e^{UN}}{\beta^{UN}}\left[\lambda^{\frac{\beta^{UN}}{2}-1} - \lambda^{-\beta^{UN}-1}\right] \tag{22}$$

$$P_{1,2}^{EB} = \frac{\mu^{EB}}{3}\left[\frac{3N^{EB} - \lambda_{cb}^2}{N^{EB} - \lambda_{cb}^2}\right]\left[\lambda - \lambda^{-5}\right] + \frac{2\mu_e^{EB}}{\beta^{EB}}\left[\lambda^{2\beta^{EB}-1} - \lambda^{-\beta^{EB}-1}\right] \tag{23}$$

$$P_1^{PS} = \frac{\mu^{PS}}{3}\left[\frac{3N^{PS} - \lambda_{cp}^2}{N^{PS} - \lambda_{cp}^2}\right]\left[\lambda - \lambda^{-3}\right] + \frac{2\mu_e^{PS}}{\beta^{PS}}\left[\lambda^{\beta^{PS}-1} - \lambda^{-\beta^{PS}-1}\right] \tag{24}$$

where $\lambda_{cu}, \lambda_{cb}, \lambda_{cp}$ are defined in Eqns (6-8). If one fits the UN, EB and PS equations to the corresponding Treloar data, the optimal material parameters are found to be:

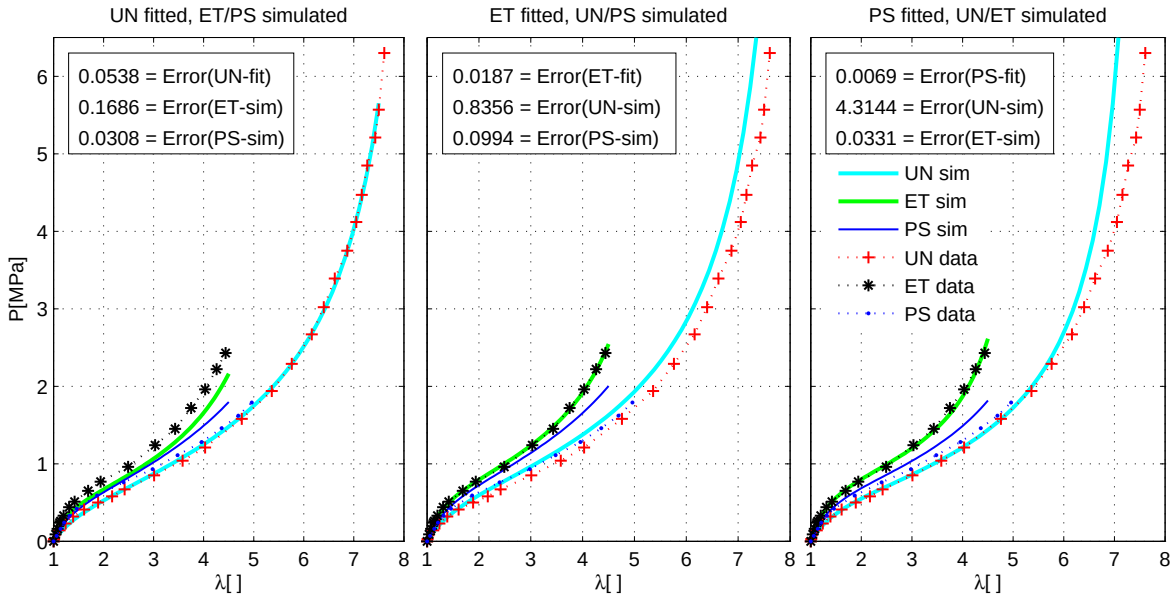

Fig. 6 Performance of the Meissner-Matějka model on the Treloar data. The fitting quality and model predictions are excellent in all deformation modes.

$$\left[\mu^{UN}, \mu_e^{UN}, N^{UN}\right] = [0.256 \text{ MPa}, 0.055 \text{ MPa}, 25.37]$$

$$\left[\mu^{EB}, \mu_e^{EB}, N^{EB}\right] = [0.270 \text{ MPa}, 0.095 \text{ MPa}, 23.47]$$

$$\left[\mu^{PS}, \mu_e^{PS}, N^{PS}\right] = [0.217 \text{ MPa}, 0.146 \text{ MPa}, 20.37]\,.$$

Concerning validity of this model, all resulting curves and corresponding errors in comparison with Treloar's data are summrized in Fig (6). It reveals excellent fitting and validity of the model in all deformation modes. During optimization for the parameter identification, an important parameter, i.e. β ($0 < \beta \leq 1$) is kept frozen ($\beta = 0.2$) as suggested by Kaliske and Heinrich [17] for better fitting and simulation of the Treloar data, even if it can be determined during parameter identification. Note that due to the presence of the constraint contribution in the energy function, the simulations for the equibiaxial case are better than the original eight-chain model. The predictions for the UN and PS cases by the EB-fitted parameters slightly overestimate the Treloar data, cf. Fig (6, **middle**). In addition, it can be noted that this model captures all deformation mode data excellently if it is compared to the similarly structured 3-parameters model, e.g. the modified Flory-Erman model or the Gornet-Desmorat (GD) model.

3.6 Bechir model

As mentioned earlier, the classical eight-chain model ignores the contribution from the entanglements-like physical cross-links during deformation of the network. To add the effects of the interactions between chains of the cross-linked network, an extra energy function, in addition to the eight-chain energy function, is appended. The free-energy of the constraint network is idealized using the standard three-chain energy function and the free-energy of the unconstrained idealized network is constructed by means of the eight-chain model. Therefore, according to Bechir et al. [33], the total free energy function of this model is merely a combination of the two chain models, i.e.

$$\begin{aligned}\Psi &= \Psi_{8ch} + \Psi_{3ch} \\ &= \mu_f N_8 \left[\lambda_{c,r}\beta + \ln\left(\frac{\beta}{\sinh\beta}\right)\right] + \frac{\mu_c N_3}{3}\sum_{j=1}^{j=3}\left[\bar{\lambda}_{rj}\bar{\beta}_j + \ln\left(\frac{\bar{\beta}_j}{\sinh\bar{\beta}_j}\right)\right]\end{aligned} \tag{25}$$

where $\beta = \mathscr{L}^{-1}(\lambda_{c,r}), \lambda_{c,r} = \sqrt{\frac{\lambda_1^2+\lambda_2^2+\lambda_3^2}{3N_8}}$ and $\bar{\beta}_j = \mathscr{L}^{-1}(\bar{\lambda}_{rj}), \bar{\lambda}_{rj} = \frac{k\lambda_j}{\sqrt{N_3}}$. In Eqn (25), $\mu_f, \mu_c, N_8, N_3, k$ are shear moduli for the free and constraint parts, numbers of chain segments for the eight and three-chain functions and a non-affine parameter, respectively. Bechir et al. [33] also proposed some relations for the material parameter set, e.g., $\mu_o = \mu_c + \mu_f$, where $\mu_c = [1 - \frac{\eta\alpha}{\sqrt{N_3}}]\mu_0$, $\mu_f = \rho\lambda_r\mu_0$, and $\alpha = \texttt{max}(\bar{\lambda}_1, \bar{\lambda}_2, \bar{\lambda}_3)$. Note that $\bar{\lambda}_i$ relate to the principal micro-stretches while λ_i are the line-stretches (continuum stretches). Evaluation of Eqn (1) provides the corresponding analytical formulations for the UN, EB and PS cases:

$$P_1^{UN} = \left[1 - \frac{\eta^{UN}\lambda_k}{\sqrt{N_3^{UN}}}\right]\frac{\mu^{UN}}{3\lambda}\left[\lambda_k^2\frac{3N_3^{UN}-\lambda_k^2}{N_3^{UN}-\lambda_k^2} - \lambda_k^{-1}\frac{3N_3^{UN}-\lambda_k^{-1}}{N_3^{UN}-\lambda_k^{-1}}\right] + \frac{\rho^{UN}\mu^{UN}\lambda_{c,ru}}{3}\left[\frac{3-\lambda_{ru}^2}{1-\lambda_{ru}^2}\right]\left[\lambda - \lambda^{-2}\right] \tag{26}$$

$$P_{1,2}^{EB} = \left[1 - \frac{\eta^{EB}\lambda_k}{\sqrt{N_3^{EB}}}\right]\frac{\mu^{EB}}{3\lambda}\left[\lambda_k^2\frac{3N_3^{EB}-\lambda_k^2}{N_3^{EB}-\lambda_k^2} - \lambda_k^{-4}\frac{3N_3^{EB}-\lambda_k^{-4}}{N_3^{EB}-\lambda_k^{-4}}\right] + \frac{\rho^{EB}\mu^{EB}\lambda_{c,rb}}{3}\left[\frac{3-\lambda_{rb}^2}{1-\lambda_{rb}^2}\right]\left[\lambda - \lambda^{-5}\right] \tag{27}$$

$$P_1^{PS} = \left[1 - \frac{\eta^{PS}\lambda_k}{\sqrt{N_3^{PS}}}\right]\frac{\mu^{PS}}{3\lambda}\left[\lambda_k^2\frac{3N_3^{PS}-\lambda_k^2}{N_3^{PS}-\lambda_k^2} - \lambda_k^{-2}\frac{3N_3^{PS}-\lambda_k^{-2}}{N_3^{PS}-\lambda_k^{-2}}\right] + \frac{\rho^{PS}\mu^{PS}\lambda_{c,rp}}{3}\left[\frac{3-\lambda_{rp}^2}{1-\lambda_{rp}^2}\right]\left[\lambda - \lambda^{-3}\right] \tag{28}$$

where $\lambda_k = k\lambda$, $\lambda_{c,ru} = \sqrt{\frac{\lambda^2+2/\lambda}{3N_8}}$, $\lambda_{c,rb} = \sqrt{\frac{2\lambda^2+1/\lambda^4}{3N_8}}$, $\lambda_{c,rp} = \sqrt{\frac{\lambda^2+1+1/\lambda^2}{3N_8}}$. Fitting UN, EB and

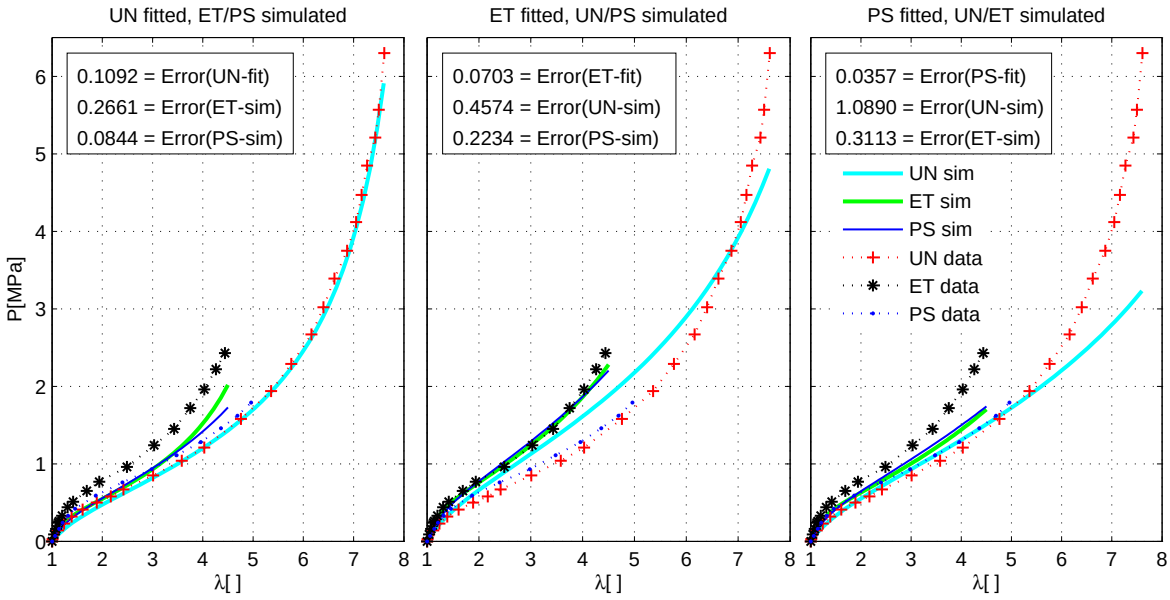

Fig. 7 Performance of the Bechir model on the Treloar data.

PS equations to the corresponding Treloar data, the optimal material parameters are obtained to be

$$\begin{aligned}\left[\mu^{UN}, \rho^{UN}, \eta^{UN}, N_3^{UN}, N_8^{UN}\right] &= [0.296 \text{ MPa}, 1.28, 1.39, 71.83, 26.01]\\ \left[\mu^{EB}, \rho^{EB}, \eta^{EB}, N_3^{EB}, N_8^{EB}\right] &= [0.251 \text{ MPa}, 1.46, 1.20, 68.20, 22.02]\\ \left[\mu^{PS}, \rho^{PS}, \eta^{PS}, N_3^{PS}, N_8^{PS}\right] &= [0.201 \text{ MPa}, 1.26, 1.02, 56.21, 20.21]\,.\end{aligned}$$

To study the model performance, each parameter set obtained from the optimization tool is used to simulate the other two deformation modes. The results are plotted in Fig (7) together with fitting and simulation errors in each case. Although, this model inherits more parameters, i.e. five in total, but it can be clearly seen that each set of optimal parameters produces simulation results for the complementary deformation modes that are not quantitatively improved than any other of the previous models of less parameters.

3.7 Wu-Giessen model

Several authors [6; 7; 14; 24] coin the term *full-network* where the chains are assumed to be randomly oriented in space for which the strain energy function is derived by integrating the response of all chains over the space. Since the numerical integration for such a full-network model is computationally costly, a weighted average is proposed by combining the three-chain and the eight-chain formulations which might provide better results than the individual three-chain or the eight-chain model [14], i.e.

$$\Psi = \Psi_{3c}[1-\rho] + \rho\Psi_{8c} \tag{29}$$

where the parameter ρ is a constant or related to some other physical quantity which is for instance related to the deformation process and Ψ_{3c}, Ψ_{8c} are energy functions for the three-chain and eight-chain models, respectively. Such form of the full-network model was proposed by Wu and Giessen [14] to improve the modelling capacity for amorphous glassy polymers, e.g. polycarbonate, where the hyperelastic energy function is used for modelling the so-called back stress. Frequently used relation for ρ is $\rho = 0.85\lambda_{\text{max}}/\sqrt{N}$, where $\lambda_{\text{max}} = \texttt{max}(\lambda_1, \lambda_2, \lambda_3)$. The factor 0.85 is chosen to provide the best correlation of Eqn (29) with numerical integration of the full-network equation. The analytical expressions for UN, EB and PS are obtained, according to the idea of the Wu and Giessen [14] model, as

$$P_1^{UN} = P_{1,3c}^{UN}[1-\rho] + \rho P_{1,8c}^{UN}, \quad P_1^{EB} = P_{1,3c}^{EB}[1-\rho] + \rho P_{1,8c}^{EB}, \quad P_1^{PS} = P_{1,3c}^{PS}[1-\rho] + \rho P_{1,8c}^{PS} \tag{30}$$

where $P_{1,8c}^{UN}, P_{1,8c}^{EB}, P_{1,8c}^{PS}$ and $P_{1,3c}^{UN}, P_{1,3c}^{EB}, P_{1,3c}^{PS}$ are UN, EB, PS stresses for the eight-chain and three-chain models, respectively. For the derivations of $P_{1,3c}^{UN}, P_{1,3c}^{EB}$, and $P_{1,3c}^{PS}$, our previous work is referred [28]. To verify the sensitivity of the model with respect to different deformation modes and also with material parameters, if the UN, EB and PS equations fit to the corresponding Treloar data, the optimal material parameters are identified:

$$\mu^{UN} = 0.318 \text{ MPa}, \qquad \mu^{EB} = 0.403 \text{ MPa}, \qquad \mu^{PS} = 0.309 \text{ MPa},$$
$$N^{UN} = 63.69, \qquad N^{EB} = 58.00, \qquad N^{PS} = 90.53.$$

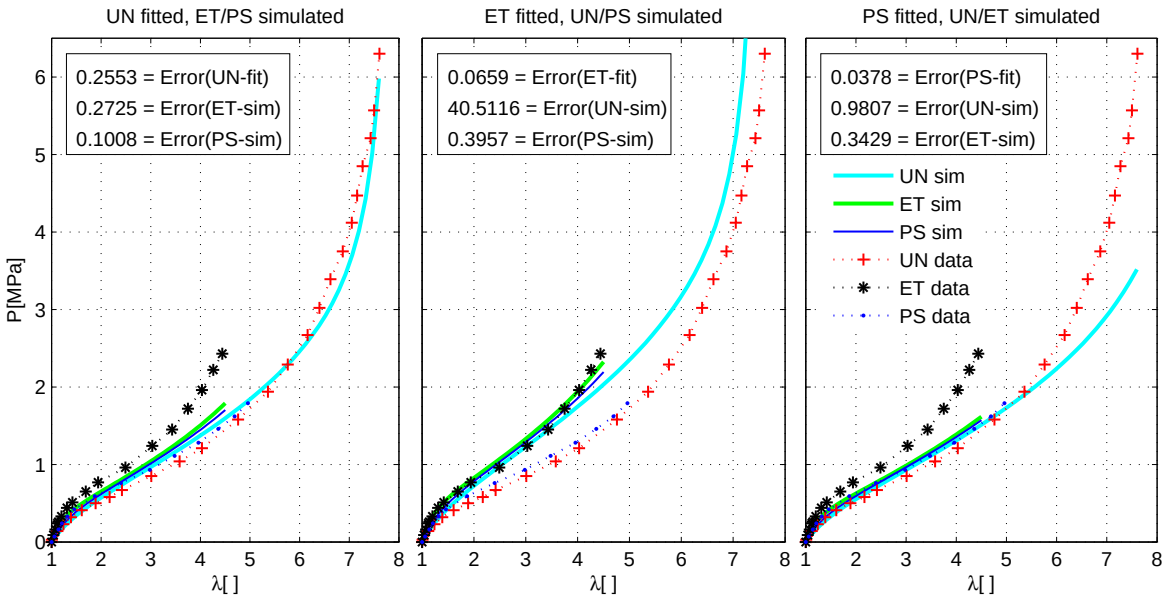

Fig. 8 Performance of the full-network model on the Treloar data.

Similar to other models, each parameter set of this model obtained from the fitting procedure is used to simulate the other two deformation modes and the corresponding errors are tabulated. The full-network model suggested by Wu and Giessen [14] predicts a biaxial stress-stretch response which falls in-between the results predicted by the eight-chain model and that predicted by the three-chain model. Aiming at better performance over the eight-chain model or the three-chain model, the capability of this model to reproduce the experimental data for all deformation modes does not show any significant improvement so far, cf. Fig (8).

3.8 Zuniga-Beatty model

Zuniga and Beatty [10] at first amend the original eight-chain and three-chain models by using a modified non-Gaussian (Kuhn-Grün) probability function in the case of energy function derivation. Jernigan and Flory [22]

show that an amended distribution function, in contrast to the Kuhn-Grün function, provides a much improved approximation to the exact result over the entire range of λ_r (relative chain stretch) values. Therefore, Zuniga and Beatty [10] re-derive the energy functions for the eight-chain and three-chain models using the amended distribution function. Then, a modified full-network model is proposed by combining the amended versions of the eight-chain and three-chain models in the line of Wu and Giessen [14] concept. Wu and Giessen [14] assume the same value for the number of chain segments, i.e. N for the eight-chain and three-chain models, which is unjustified due to inherent geometrical considerations of these two models. Hence, Zuniga and Beatty [10] propose separate values for N, i.e. N_3, N_8 for the three-chain and eight-chain models, respectively. Due to the amended form for the probability function, the energy functions of the eight-chain and three-chain models are as follows

$$\Psi_{8c} = \mu \left[N_8 \left[\lambda_{c,r}\beta + \ln\left(\frac{\beta}{\sinh\beta}\right)\right] - \ln\left(\frac{\beta}{\lambda_r}\right)\right] \tag{31}$$

and

$$\Psi_{3c} = \frac{\mu}{3}\sum_{j=1}^{j=3}\left[N_3 \left[\lambda_{rj}\beta_j + \ln\left(\frac{\beta_j}{\sinh\beta_j}\right)\right] - \ln\left(\frac{\beta_j}{\lambda_{rj}}\right)\right]. \tag{32}$$

In Eqns (31) and (32), $\lambda_{c,r} = \sqrt{\frac{I_1}{3N_8}}, \beta = \mathscr{L}^{-1}(\lambda_{c,r}), \beta_j = \mathscr{L}^{-1}(\lambda_{rj}), \lambda_{rj} = \frac{\lambda_j}{\sqrt{N_3}}$, where I_1 and $\lambda_{c,r}$ are defined in Section 3.1. Hence, the modified form of the full-network energy function proposed by Zuniga and Beatty [10] is

$$\Psi = [1-\rho_{3c}]\Psi_{3c} + \rho_{8c}\Psi_{8c} \tag{33}$$

where

$$\rho_{3c} = \frac{a\Lambda_L}{\sqrt{N_3}}, \quad \rho_{8c} = \frac{b\Lambda_c}{\sqrt{N_8}}. \tag{34}$$

In Eqn (34), Λ_L is related to the principal stretches through the state of deformation to which the continuum is subjected so that the greater stretch $\lambda_1 = \Lambda_L$ and the chain stretch for the eight-chain model is $\Lambda_c = \sqrt{\frac{\lambda_1^2+\lambda_2^2+\lambda_3^2}{3}}$ while a, b are two positive scaling factors. However, for simplicity, they choose to follow $a = b = 1$, see Zuniga and Beatty [10] for details. The analytical formulations for the UN, EB and PS for this composite model are

$$P_1^{UN} = P_{1,3cm}^{UN}\left[1 - \frac{\lambda}{\sqrt{N_3^{UN}}}\right] + \frac{\lambda_{cu}}{\sqrt{N_8^{UN}}} P_{1,8cm}^{UN} \tag{35}$$

$$P_1^{EB} = P_{1,3cm}^{EB}\left[1 - \frac{\lambda}{\sqrt{N_3^{EB}}}\right] + \frac{\lambda_{cb}}{\sqrt{N_8^{EB}}} P_{1,8cm}^{EB} \tag{36}$$

$$P_1^{PS} = P_{1,3cm}^{PS}\left[1 - \frac{\lambda}{\sqrt{N_3^{PS}}}\right] + \frac{\lambda_{cp}}{\sqrt{N_8^{PS}}} P_{1,8cm}^{PS} \tag{37}$$

where the expressions for $P_{1,3cm}^{UN}, P_{1,3cm}^{EB}, P_{1,3cm}^{PS}, P_{1,8cm}^{UN}, P_{1,8cm}^{EB}, P_{1,8cm}^{PS}$ can be obtained from Appendix B and $\lambda_{cu}, \lambda_{cb}, \lambda_{cp}$ are defined in Eqns (6-8). The optimal parameter sets for this model are estimated as

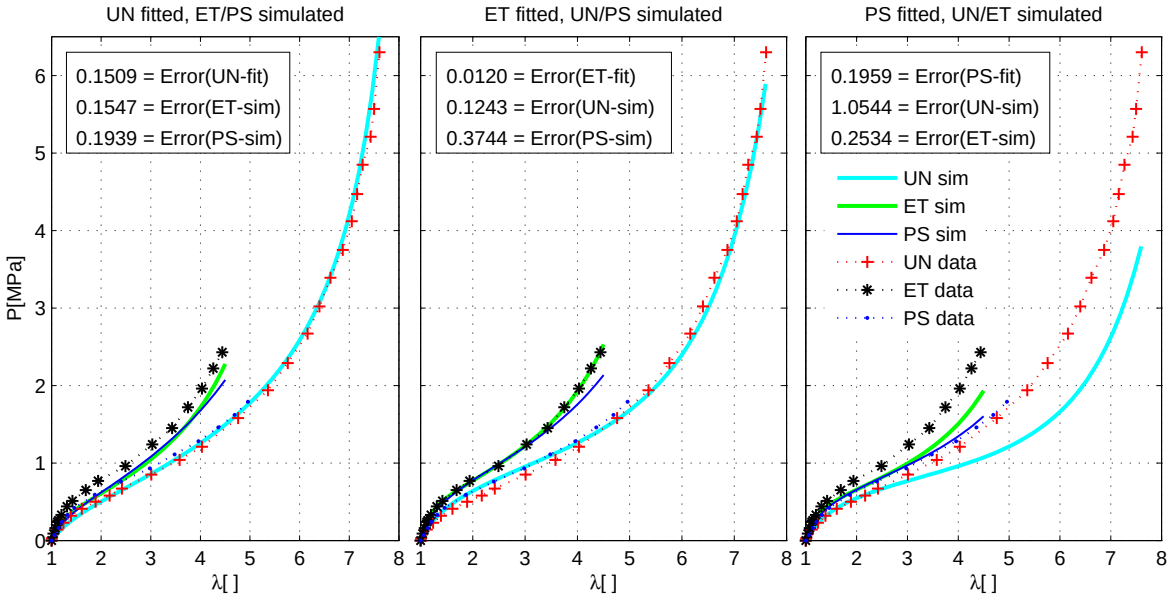

Fig. 9 Performance of the Zuniga-Beatty version of the full-network model on the Treloar data. The fitting and simulations in all deformation modes are excellent except an underestimation occurs in the case of UN data for the PS-fitted parameters.

$$\mu^{UN} = 0.27 \text{ MPa}, \qquad \mu^{EB} = 0.48 \text{ MPa}, \qquad \mu^{PS} = 0.45 \text{ MPa},$$

$$N_3^{UN} = 75.13, \qquad N_3^{EB} = 8.8, \qquad N_3^{PS} = 6.55,$$

$$N_8^{UN} = 25.12, \qquad N_8^{EB} = 28.55, \qquad N_8^{PS} = 31.49.$$

Concerning the validity of the model, the parameter set obtained from the optimization tool in each deformation case is used to simulate the other two deformation modes. The results are plotted in Fig (9) together with fitting and simulation errors in each case. The fittings and simulations for UN- and EB-fitted parameters are good to excellent in predicting the data for other deformation modes except a small overestimation is observed for the PS data. It can be clearly stated here that with an additional parameter, the Zuniga-Beatty

version of the full-network shows better performance than the Wu-Giessen version. The reason might be that (a) Zuniga-Beatty used an improved version of the probability function and (b) the scaling factor (ρ, in the original version of Wu-Giessen model) is replaced by a deformation-dependent stretch, cf. Eqn (34).

4 Conclusion

In this paper, a comparative study on the classical eight-chain and full-network models and six of their modified versions is presented. Some of the modified versions are of phenomenological types while others are originated from the micro-mechanics of chain molecules. In order to perform the comparative study, the analytical formulations in the case of three different deformation modes of the eight selected models are derived. Then, the performance evaluation is highlighted of all selected models in reproducing the classical experimental data of Treloar. This study demonstrates that the two-parameter bootstrapped eight-chain model predicts the Treloar data better than the classical eight-chain model. Note that several constitutive models, e.g. the modified Flory-Erman model, the Meissner-Matějka model, the GD model which consider constraint contribution in deriving their free energy functions predict all three deformation modes quite reasonable than the classical eight-chain model. However, the Bechir model with five parameters does not show improved results in comparison to the original eight-chain model. In the case of full-network model, the Zuniga-Beatty version with an improved probability function for chain statistics shows better performance than the Wu-Giessen form of full-network model. Such performance analysis will help a design engineer or a beginnner in rubber mechanics to choose whether the classical eight-chain model or full-network model or one of their modified versions is appropriate from a considerable number of rubber-like material models available in the literature.

Appendix A: Derivatives of the Flory-Erman energy function (constraint part)

To derive the analytical formulations for different defomation modes, the single derivatives of the energy function (constraint part) of the Flory-Erman model expressed in principal stretches are essential, i.e.

$$\frac{\partial \Psi_{ct}}{\partial \lambda_i} = \frac{2\kappa^2[\lambda_i^2-1][\kappa^4+\kappa^3\lambda_i^4-\kappa^3\lambda_i^2+2\kappa^3+2\kappa^2\lambda_i^4+2\kappa\lambda_i^6+\lambda_i^6]}{\lambda_i[[\lambda_i^2+\kappa]^2][\kappa^4+\kappa^3\lambda_i^4+\kappa^3\lambda_i^2+2\kappa^3+3\kappa^2\lambda_i^4+3\kappa^2\lambda_i^2+\kappa\lambda_i^6+3\kappa\lambda_i^4+\lambda_i^6]}. \tag{38}$$

Appendix B: Analytical expressions for the amended three-chain and eight-chain models

The analytical expressions for the amended three-chain and eight-chain models for different deformation modes, i.e. UN, EB and PS are as follows,

Uniaxial tension (UN):

$$P_{1,3cm}^{UN} = \frac{\mu^{UN}\sqrt{N_3^{UN}}}{3}\left[\beta_1 - \frac{\beta_2}{\lambda^{3/2}} + \frac{1}{\lambda^{3/2}N_3^{UN}\beta_2[1-\frac{1}{\lambda N_3^{UN}}-\frac{2}{\beta_2\sqrt{\lambda N_3^{UN}}}]} - \frac{1}{N_3^{UN}\beta_1[1-\frac{\lambda^2}{N_3^{UN}}-\frac{2\lambda}{\beta_1\sqrt{N_3^{UN}}}]}\right]$$

$$P_{1,8cm}^{UN} = \frac{\mu^{UN}[\lambda-\lambda^{-2}]}{3\lambda_{c,r}}\left[\beta + \frac{1}{N_8^{UN}\lambda_{c,r}} - \frac{1}{N_8^{UN}\beta[1-\lambda_{c,r}^2-\frac{2\lambda_{c,r}}{\beta}]}\right]$$

where, $\lambda_{c,r} = \sqrt{\frac{1}{3N_8^{UN}}\left[\lambda^2+\frac{2}{\lambda}\right]}, \beta = \lambda_{c,r}\frac{3-\lambda_{c,r}^2}{1-\lambda_{c,r}^2}, \beta_1 = \frac{\lambda}{\sqrt{N_3^{UN}}}\frac{3N_3^{UN}-\lambda^2}{N_3^{UN}-\lambda^2}, \beta_2 = \frac{1}{\sqrt{\lambda N_3^{UN}}}\frac{3N_3^{UN}\lambda-1}{N_3^{UN}\lambda-1}.$

Equibiaxial tension (EB):

$$P_{1,3cm}^{EB} = \frac{\mu^{EB}\sqrt{N_3^{EB}}}{3}\left[\beta_1 - \frac{\beta_3}{\lambda^3} + \frac{1}{N_3^{EB}\beta_3[\lambda^3-\frac{1}{\lambda N_3^{UN}}-\frac{2\lambda}{\beta_3\sqrt{N_3^{EB}}}]} - \frac{1}{N_3^{EB}\beta_1[1-\frac{\lambda^2}{N_3^{EB}}-\frac{2\lambda}{\beta_1\sqrt{N_3^{EB}}}]}\right]$$

$$P_{1,8cm}^{EB} = \frac{\mu^{EB}[\lambda-\lambda^{-5}]}{3\lambda_{c,r}}\left[\beta + \frac{1}{N_8^{EB}\lambda_{c,r}} - \frac{1}{N_8^{EB}\beta[1-\lambda_{c,r}^2-\frac{2\lambda_{c,r}}{\beta}]}\right]$$

where, $\lambda_{c,r} = \sqrt{\frac{1}{3N_8^{EB}}\left[2\lambda^2+\frac{1}{\lambda^4}\right]}, \beta = \lambda_{c,r}\frac{3-\lambda_{c,r}^2}{1-\lambda_{c,r}^2}, \beta_1 = \frac{\lambda}{\sqrt{N_3^{EB}}}\frac{3N_3^{EB}-\lambda^2}{N_3^{EB}-\lambda^2}, \beta_3 = \frac{\lambda^{-2}}{\sqrt{N_3^{EB}}}\frac{3N_3^{EB}-\lambda^{-4}}{N_3^{EB}-\lambda^{-4}}.$

Pure shear (PS):

$$P_{1,3cm}^{PS} = \frac{\mu^{PS}\sqrt{N_3^{PS}}}{3}\left[\beta_1 - \frac{\beta_4}{\lambda^2} + \frac{1}{N_3^{PS}\beta_4[\lambda^2-\frac{1}{N_3^{PS}}-\frac{2\lambda}{\beta_4\sqrt{N_3^{PS}}}]} - \frac{1}{N_3^{PS}\beta_1[1-\frac{\lambda^2}{N_3^{PS}}-\frac{2\lambda}{\beta_1\sqrt{N_3^{PS}}}]}\right]$$

$$P_{1,8cm}^{PS} = \frac{\mu^{PS}[\lambda-\lambda^{-3}]}{3\lambda_{c,r}}\left[\beta + \frac{1}{N_8^{PS}\lambda_{c,r}} - \frac{1}{N_8^{PS}\beta[1-\lambda_{c,r}^2-\frac{2\lambda_{c,r}}{\beta}]}\right]$$

where, $\lambda_{c,r} = \sqrt{\frac{1}{3N_8^{PS}}[\lambda^2+\lambda^{-2}+1]}, \beta = \lambda_{c,r}\frac{3-\lambda_{c,r}^2}{1-\lambda_{c,r}^2}, \beta_1 = \frac{\lambda}{\sqrt{N_3^{PS}}}\frac{3N_3^{PS}-\lambda^2}{N_3^{PS}-\lambda^2}, \beta_4 = \frac{\lambda^{-1}}{\sqrt{N_3^{PS}}}\frac{3N_3^{PS}-\lambda^{-2}}{N_3^{PS}-\lambda^{-2}}.$

References

1. Amin AFMS (2001) Constitutive modeling of strain-rate dependency of natural and high damping rubbers, PhD Dissertation, Saitama University, Japan
2. Amin AFMS, Wiraguna SI, Bhuiyan AR, Okui Y (2006a) Hyperelasticity model for finite element analysis of natural and high damping rubbers in compression and shear. Journal of Engineering Mechanics ASCE 132(1): 54-64
3. Amin AFMS, Lion A, Sekita S, Okui Y (2006) Nonlinear dependence of viscosity in modeling the rate-dependent response of natural and high damping rubbers in compression and shear: Experimental identification and numerical verification. International Journal of Plasticity 22: 1610-1657
4. Milani G, Milani F (2012) Stretch-stress behavior of elastomeric seismic isolators with different rubber materials: Numerical insight. Journal of Engineering Mechanics ASCE 138(5): 416-428

5. Treloar LRG (1944) Stress-strain data for vulcanised rubber under various types of deformation. Transactions of the Faraday Society 40: 59-70
6. Treloar LRG, Riding G (1979) A non-Gaussian theory of rubber in biaxial strain. I. Mechanical properties. Proceedings of the Royal Society of London. A369, 1979, p.261
7. Beatty MF (2003) An average-stretch full-network model for rubber elasticity. Journal of Elasticity 70: 65-86
8. Miehe C, Göktepe S, Lulei F (2004) A micro-macro approach to rubber-like materials - Part I: The non-affine micro-sphere model of rubber elasticity. Journal of the Mechanics and Physics of Solids 52: 2617-2660
9. Boyce MC, Arruda EM (2000) Constitutive models of rubber elasticity: a review. Rubber Chemistry and Technology 73: 504-523,2000
10. Elias-Zuniga A, Beatty MF (2002) Constitutive equations for amended non-Gaussian network models of rubber elasticity. International Journal of Engineering Science 40: 2265-2294
11. Arruda EM, Boyce MC (1993) A three-dimensional constitutive model for the large stretch behavior of rubber elastic materials. Journal of the Mechanics and Physics of Solids 41: 389-412
12. Ogden RW (1972) Large deformation isotropic elasticity - on the correlation of theory and experiment for incompressible rubberlike solids. Proceedings of the Royal Society of London. Series A, Mathematical and Physical Sciences 326: 565-584
13. Ogden RW, Saccomandi G, Sgura I (2004) Fitting hyperelastic models to experimental data. Computational Mechanics 34: 484-502
14. Wu PD, van der Giessen E (1992) On improved 3-D non-Gaussian network models for rubber elasticity. Mechanics Research Communications 19: 427-433
15. Kroon M (2011) An 8-chain model for rubber-like materials accounting for non-affine chain deformations and topological constraints. Journal of Elasticity 102 (2): 99-116, 2011,
16. Marckmann G, Verron E (2006) Comparison of hyperelastic models for rubber-like materials. Rubber Chemistry and Technology 79: 835-858
17. Kaliske M, Rothert H (1997) On the finite element implementation of rubber-like materials at finite strains. Engineering Computations 14: 216-232
18. Kaliske M, Heinrich G (1999) An extended tube-model for rubber elasticity: Statistical mechanical theory and finite element implementation. Rubber Chemistry and Technology 72: 602-632
19. Chagnon G, Marckmann G, Verron E (2004) A comparison of the Hart-Smith model with Arruda-Boyce and Gent formulations for rubber elasticity. Rubber Chemistry and Technology 77: 724-735
20. Hart-Smith LJ (1966) Elasticity parameters for finite deformations of rubber like materials. Zeitschrift für Angewandte Mathematik und Physik 17: 608-626
21. Flory PJ, Erman B (1980) Theory of elasticity of polymer networks 3. Macromolecules 15(3): 800-806
22. Jernigan, RL, Flory PJ (1969) Distribution functions for chain molecules. Journal of Chemical Physics 50: 4185-4201
23. Shariff MHBM (2000) Strain energy function for filled and unfilled rubber-like material. Rubber Chemistry and Technology 73: 1-18
24. Elias-Zuniga A (2006) A non-Gaussian network model for rubber elasticity. Polymer 47: 907-914
25. Pucci E, Saccomandi G (2002) A note on the Gent model for rubber-like materials. Rubber Chemistry and Technology 75(5):839-851
26. Hossain M, Steinmann P (2013) More hyperelastic models for rubber-like materials: Consistent tangent operator and comparative study. Journal of the Mechanical Behaviour of Materials 22(1-2):27-50
27. Hossain M, Vu D K, Steinmann P (2012) Experimental study and numerical modelling of VHB 4910 polymer. Computational Materials Science 59:65-74

28. Steinmann P, Hossain M, Possart G (2012) Hyperelastic models for rubber-like materials: Consistent tangent operators and suitability for Treloar's data. Archive of Applied Mechanics, DOI:10.1007/s00419-012-0610-z
29. Morini B, Porcelli M (2010) TRESNEI, a Matlab trust-region solver for systems of nonlinear equalities and inequalities. Computational Optimization and Applications, DOI: 10.1007/s10589-010-9327-5
30. Jerrams S, Murphy N (Editors) Constitutive models for rubber VII. Proceedings of the 7th european conference on constitutive models for rubber, Dublin, Ireland. CRC Press (Taylor & Francis Group), 2012
31. Miroshnychenko D, Green WA, Turner DM (2005) Composite and filament models for the mechanical behaviour of elastomeric materials. Journal of the Mechanics and Physics of Solids 53:748-770
32. Miroshnychenko D, Green WA (2009) Heuristic search for a predictive strain-energy function in nonlinear elasticity. International Journal of Solids and Structures 46:271-286
33. Bechir H, Chevalier L, Idjeri M (2010) A three-dimensional network model for rubber elasticity: The effect of local entanglements constraints. International Journal of Engineering Science 48: 265-274
34. Meissner B, Matejka L (2003) A Langevin-elasticity-theory-based constitutive equation for rubberlike networks and its comparison with biaxial stress-strain data. Part I. Polymer 44: 4599-4510
35. Meissner B, Matejka L (2004) A Langevin-elasticity-theory-based constitutive equation for rubberlike networks and its comparison with biaxial stress-strain data. Part II. Polymer 45: 7247-7260
36. Itskov M, Ehret AE, Dargazany R (2010) A full-network rubber elasticity model based on analytical integration. Mathematics and Mechanics of Solids 15: 655-671
37. Sahu R K, Patra K (2013) Estimation of elastic modulus of dielectric elastomer materials using Mooney-Rivlin and Ogden Models. Advanced Materials Research 685: 331-335